Proceedings of the ASME 2020
Dynamic Systems and Control Conference
DSCC2020
October 5-7, 2020, Virtual, Online

DSCC2020-3176

EFFECT OF ELECTROMECHANICAL COUPLING ON LOCALLY RESONANT METASTRUCTURES FOR SIMULTANEOUS ENERGY HARVESTING AND VIBRATION ATTENUATION APPLICATIONS

Mohammad A. Bukhari
Department of Mechanical Engineering
Virginia Tech, Blacksburg, Virginia 24061
Email: bukhari@vt.edu

Feng Qian
Department of Mechanical Engineering
Virginia Tech, Blacksburg, Virginia 24061
Email: fengqian@vt.edu

Oumar R. Barry*
Department of Mechanical Engineering
Virginia Tech, Blacksburg, Virginia 24061
Email: obarry@vt.edu

Lei Zuo
Department of Mechanical Engineering
Virginia Tech, Blacksburg, Virginia 24061
Email: leizuo@vt.edu

ABSTRACT

The study of simultaneous energy harvesting and vibration attenuation has recently been the focus in many acoustic metamaterials investigations. The studies have reported the possibility of harvesting electric power using electromechanical coupling; however, the effect of the electromechanical resonator on the obtained bandgap's boundaries has not been explored yet. In this paper, we investigate metamaterial coupled to electromechanical resonators to demonstrate the effect of electromechanical coupling on the wave propagation analytically and experimentally. The electromechanical resonator is shunted to an external load resistor to harvest energy. We derive the analytical dispersion curve of the system and show the band structure for different load resistors and electromechanical coupling coefficients. To verify the analytical dispersion relations, we also simulate the system numerically. Furthermore, experiment is carried out to validate the analytical observations. The obtained observations can guide designers in selecting electromechanical resonator parameters for effective energy harvesting from metamaterials.

*Address all correspondence to this author.

INTRODUCTION

Unlike homogeneous structures, artificially structured crystals in special engineered configurations and patterns can exhibit a superior vibration control performance particularly at low frequencies. These structures are called metamaterials [1, 2]. For instance, arranging crystals in periodic configuration can attenuate waves with wavelength near the lattice constant from propagating through the structure. This phenomena is also known as Bragg scattering [3–8].

Controlling smaller structures with lattice constant much smaller than the wavelength can be obtained by embedding local resonators inside the structure to form locally resonant metamaterials [9]. This is a consequence of mode hybridization. Nevertheless, Bragg scattering can still be observed in locally resonant metamaterials [10]. Formation of bandgaps in locally resonant metamaterials depend on the local resonator's parameters [11].

By attaching a piezoelectric patch on the local resonator, electromechanical bandgap can be formed due to the added stiffness to the system by the electromechanical coupling [12–16]. Moreover, shunting the piezoelectric patch to an external resistor can harvest the kinetic energy from wave propagating through the structure [17]. This offers simultaneous energy harvesting and vibration attenuation in metamaterials. Inspiring by meta-

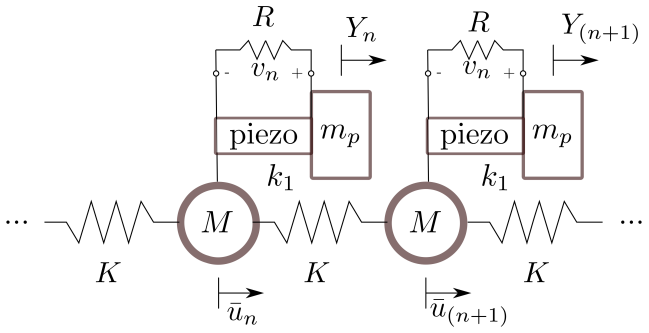

FIGURE 1: A schematic diagram for the locally electromechanical resonant metamaterial.

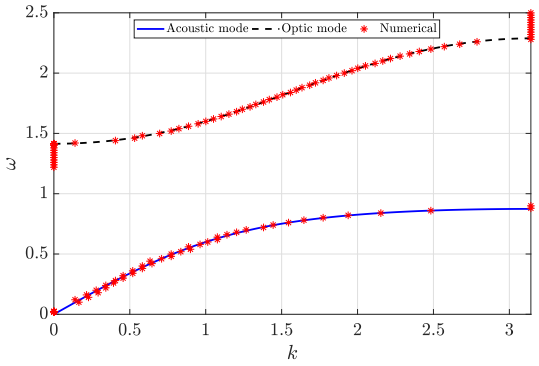

FIGURE 2: Analytical and numerical band structures for a chain with electromechanical resonator: $\omega_d = \omega_n = 1000$ rad/s^2, $k_1 = 10^6$ N/m, $\bar{k} = 1$, $\theta = 10^{-10}$ N/V, $C_p = 13.3 \times 10^{-9}$, and $R = 10^7\Omega$.

materials' flat frequency response [18], many researcher investigated energy harvesting from local electromechanical resonators. This included models for discrete crystals [17] and distributed parameter metamaterials [19]. Moreover, Hu et al., [20] suggested coupling the local resonators in metamaterials to enhance the energy harvesting performance. Furthermore, experimintal demonstration for energy harvesting and vibration attenuation in 3D printed 2D structure can be found in [21]. Another application for 2D metamaterials in energy harvesting is focusing propagating waves by lens for effective energy harvesting [22].

The aforementioned investigations have examined the concept of energy harvesting from metamaterials with electromechanical resonators. However, there were no studies that examines the effect of electromechanical coupling with load resistor on the band structure of locally resonant metamaterials. It is also unknown whether the energy harvesting degrades the performance of vibration attenuation in metastructure. This is the focus of the current study. In this paper, we examine the wave propagation in a chain with local electromechanical resonators. The electromechanical resonator is shunted to an external load resistor to harvest the generated power. We present the governing equation of motions and then obtain the dispersion relation analytically. We also validate the obtained analytical results numerically. Moreover, we investigate the influence of different electromechanical coupling parameters on the band structure. Finally, we experimentally validate the observed analytical results with a finite structure.

SYSTEM DESCRIPTION AND MATHEMATICAL MODELING

A schematic diagram for the locally electromechanical resonant chain is shown in Fig. 1. s periodic crystals with a mass, M, lattice constant, a, and connected by a linear spring with a coefficient, K. A local electromechanical resonator shunted to an external resistor R is embedded in each cell. The electromechanical resonator has an effective mass, m_p, effective stiffness, k_1, electromechanical coupling coefficient, θ, and capacitance of the piezoelectric element, C_p. The displacement of the n^{th} cell is $\bar{u}_n$, the absolute displacement of the local resonator is Y_n, and the harvested voltage by the shunted resistor is $\bar{v}_n$.

The governing equation of motions for the n^{th} crystal and its electromechanical local resonator can be expressed as

$$M\ddot{\bar{u}}_n + 2K\bar{u}_n - K\bar{u}_{n+1} - K\bar{u}_{n-1} + m_p(\ddot{\bar{y}}_n + \ddot{\bar{u}}_n) = 0 \quad (1)$$

$$m_p\ddot{\bar{y}}_n + k_1\bar{y}_n - \theta\bar{v}_n = -m_p\ddot{\bar{u}}_n \quad (2)$$

$$RC_p\dot{\bar{v}}_n + \bar{v}_n + R\theta\dot{\bar{y}}_n = 0 \quad (3)$$

where $\bar{y}_n = Y_n - \bar{u}_n$ is the net displacement of the n^{th} electromechanical resonator, and the dots are the time derivatives.

Equations (1)-(3) can be rewritten in the dimensionless form as

$$\ddot{u}_n + 2u_n - u_{n+1} - u_{n-1} + \bar{k}\Omega_0^2(\ddot{y}_n + \ddot{u}_n) = 0 \quad (4)$$

$$\Omega_0^2\ddot{y}_n + y_n - \alpha_1 v_n = -\Omega_0^2\ddot{u}_n \quad (5)$$

$$\alpha_2\dot{v}_n + v_n + \alpha_3\dot{y}_n = 0 \quad (6)$$

where

$$\omega_n^2 = K/M, \omega_d^2 = k_1/m_p, \bar{k} = k_1/m_p, u_n = \bar{u}_n/U_0,$$
$$y_n = \bar{y}_n/y_0, v_n = \bar{v}_n/V_0, \Omega_0 = \omega_n/\omega_d, \alpha_1 = \theta V_0/k_1, \quad (7)$$
$$\alpha_2 = RC_p\omega_n, \alpha_3 = R\theta\omega_n y_0/V_0, \tau = \omega_n t$$

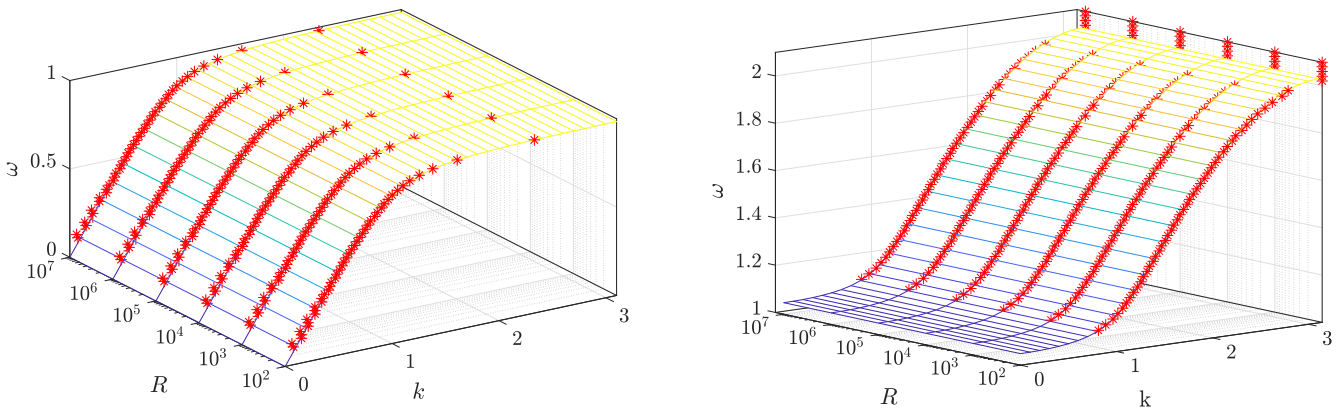

FIGURE 3: The effect of load resistor on the band structure: $\omega_d = \omega_n = 1000$ rad/s^2, $k_1 = 10^6$ N/m, $\bar{k} = 1$, $\theta = 10^{-10}$ N/V, $C_p = 13.3 \times 10^{-9}$, and $R = 10^2 - 10^7 \Omega$. (a): Acoustic mode; (b): Optical mode.

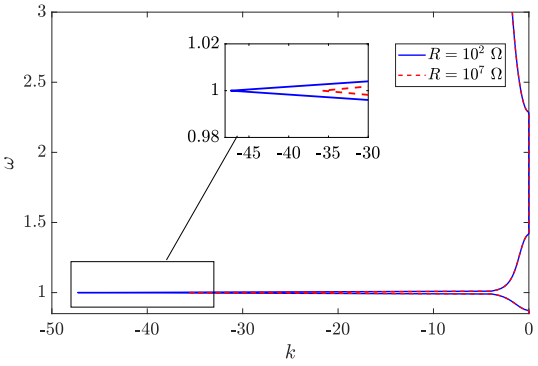

FIGURE 4: Imaginary part of the band structures for a chain with electromechanical resonator: $\omega_d = \omega_n = 1000$ rad/s^2, $k_1 = 10^6$ N/m, $\bar{k} = 1$, $\theta = 10^{-10}$ N/V, and $C_p = 13.3 \times 10^{-9}$ F.

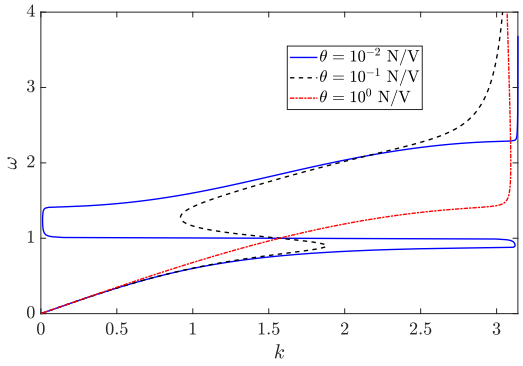

FIGURE 5: The effect of the electromechanical coupling coefficient on the band structures for a chain with electromechanical resonator: $\omega_d = \omega_n = 1000$ rad/s^2, $k_1 = 10^6$ N/m, $\bar{k} = 1$, $R = 10^2\Omega$, and $C_p = 13.3 \times 10^{-9}$ F.

and U_0, y_0, and v_0, are normalized constants. The solution of the system can be expressed as

$$u_n = Ae^{i(nk-\omega\tau)} \tag{8}$$

$$y_n = Be^{i(nk-\omega\tau)} \tag{9}$$

$$v_n = Ce^{i(nk-\omega\tau)} \tag{10}$$

where ω is angular frequency and k is the normalized wavenumber.

Introducing Eqns. (9)-(10) into Eqn. (6) yields

$$-i\alpha_2\omega C + C - i\alpha_3\omega B = 0 \tag{11}$$

Rearranging Eqn. (11) leaves us with

$$C = \Gamma B \tag{12}$$

where Γ is complex and defined as

$$\Gamma = \frac{i\alpha_3\omega}{1 - i\alpha_2\omega} \tag{13}$$

Similarly, introducing Eqns. (8)-(10) and Eqn. (12) in Eqn. (5) leads to

$$B = K_\omega A \tag{14}$$

where K_ω is also complex and defined as

$$K_\omega = \frac{\Omega_0^2 \omega^2}{1 - \alpha_1 \Gamma - \Omega_0^2 \omega^2} \tag{15}$$

By substituting Eqns. (8)-(9), and Eqn. (14), the dispersion relation of the system can be written as

$$-\omega^2 + (2 - 2\cos k) - \bar{k}\Omega_0^2 \omega^2 (1 + K_\omega) = 0 \tag{16}$$

EFFECT OF ELECTROMECHANICAL COUPLING ON THE BAND STRUCTURE

Upon calculating the roots of Eqn. (16) at a specific wave number, we get four complex roots with nonzero real part and one pure complex root. Two of the former are the passband positive frequencies while the other two roots are the passband negative frequencies. The fifth root is the frequency inside the bandgap. We plot the band structure of the system in Fig. 2. To check the accuracy of the analytical solution, we also plot the band structure obtained numerically in Fig. 2. The band structure can be obtained by numerically integrating a chain (i.e we use here 100 cells) excited at the middle point (at n = 50) by a harmonic force. Then, we determine the wave number by picking the maximum value of the 2-D spectrum; such that, the wave number is associated with the spatial frequency at the excitation frequency. To eliminate any reflected waves, the end condition is chosen to be a perfectly matched layer (PML) [23]. The numerical results shows a very good agreement with the analytical results in the presence of electromechanical coupling.

Next, we study the effect of load resistor on the band structure in a weakly electromechanical coupling case. Figure 3 shows the acoustic and optical modes for different load resistor (star lines) as compared to the case of mechanical local resonator without electromechanical coupling (mesh surface). The results indicate that neither the acoustic nor the optical mode are evidently affected by the electromechanical coupling. This indicates that metastructures can be used for simultaneous energy harvesting and vibration mitigation without degrading the bandgap boundary when the electromecanical coupling is weak. Moreover, installing piezoelectric patches on few local resonators can offer feasible energy harvesting in finite structures while preserving the vibration mitigation performance.

Although shunting the local resonator to a load resistor does not change the bandgap's size, the load resistor affects the attenuation level inside the bandgap. This can be observed from the change in the imaginary part of the band structure as shown in Fig. 4.

For stronger electromechanical coupling coefficient θ, electromechanical coupling does not also change the shape of the band structure for $\theta \leq 10^{-3}$. However, increasing the electromechanical coupling further results in gradual deformation in the band structure. Indeed, the acoustic and optical modes starts emerging into a one dispersion curve as shown in Fig. 5. Therefore, the bandgap eventually disappears. It is noteworthy here that this observation in the bandgap is not feasible in most engineering applications since the electromechanical coupling coefficient depends on the piezoelectric coefficient which does not usually exceed the order of 10^{-10} [24].

EXPERIMENTAL VALIDATIONS

In this section, experiments are carried out to study the effect of energy harvesting on the vibration attenuation performance in a finite chain with electromechanical resonators as shown in Fig. 7. The finite chain consists of five unit cells and is implemented by an aluminum clamped free beam with length of 500 mm. The beam has a modulus of elasticity of 69 GPa, 25.4 mm width, a density of 2.7 g/cm^3, and a thickness of 3.25 mm. A local eletromechanical beam resonator is attached to each cell. The beam resonator is made of copper (i.e., has a 117.2 GPa modulus of elasticity and 8.912 g/cm^3 density) to obtain high mass ratio, which has a length of 85 mm, width of 16 mm, and thickness of 2 mm. Each beam resonator is sandwiched by two piezoelectric layers that stretched over 25 mm for the resonator length and polarized in the direction of the thickness. The piezoelectric layers are bounded to the copper resonator by an electric conductive adhesive.

The finite structure was mounted on an electromagnetic shaker (VG-100) to excite the beam in the transverse direction. The shaker was driven by a Spider 80X dynamic analyzer (Crystal Instruments Inc.). The analyzer generates a closed loop controlled signal that has a constant excitation amplitude at different frequencies. The input excitation was recorded by an accelerometer (PCB356A16) and fed the closed loop controller. Another accelerometer was attached to the free end to record the output vibration. Each electromechanical resonator was shunted to a load resistor with different values ranging from the short circuit condition to the open circuit condition. The vibration of the free end along with the harvested voltage from each resonator were collected by the analyzer. The system was excited by a harmonic frequency sweep over the range of (20-300 Hz) with 0.1 g excitation amplitude. Within this frequency range, the analytical bandgap, bare structure, and electromechanical resonance frequency resonators are located.

To Validate the target frequencies for the host beam and the local resonators, we test these components using the same experimental setup. The 2^{nd}-4^{th} natural frequencies for the host beam are analytically determined as 66.4 Hz, 186.1 Hz, 366 Hz, respectively while the experimental results indicate that the corresponding frequencies are 63 Hz, 180.5 Hz, and 353 Hz, respectively. On the other hand, the natural frequency of the open

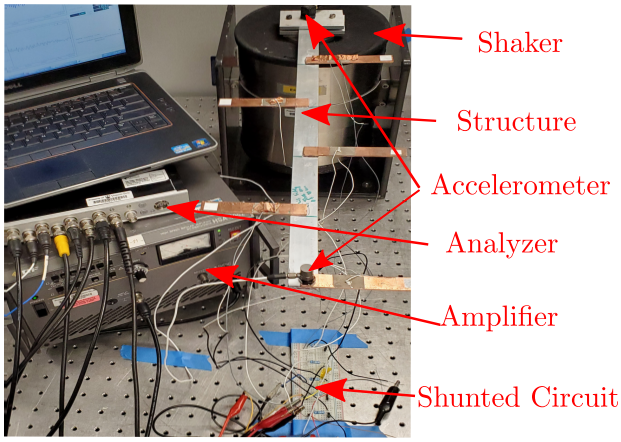

FIGURE 6: The experimental setup, a cantilever beam with 5 resonators.

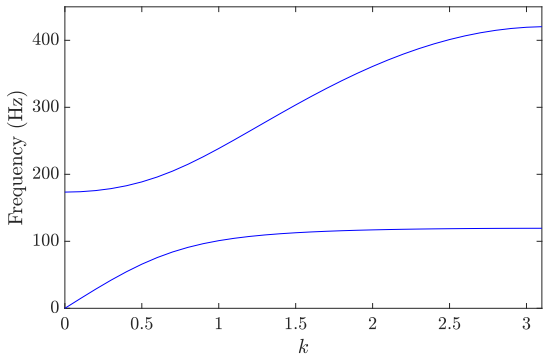

FIGURE 7: Analytical band structures for a chain with electromechanical resonator with parameters in the experimental setup: $\omega_d = 790$, $\omega_n = 1266$ rad/s^2, $k_1 = 6.788 \times 10^5$, $\bar{k} = 0.3581$.

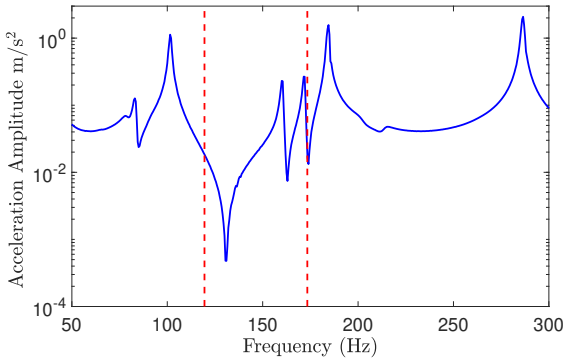

FIGURE 8: Vibration frequency response curve for a chain with electromechanical resonator with parameters in the experimental setup: $\omega_d = 790$, $\omega_n = 1266$ rad/s^2, $k_1 = 6.788 \times 10^5$, $\bar{k} = 0.3581$. Analytical bandgap is highlighted between the two vertical lines.

circuit local resonator is analytically determined as 163 Hz while the experimental results show that the local resonator frequency is 158 Hz. The errors between the analytical and numerical results are less than 5% for all measurements, these error can be explained by the added mass from the accelerometer at the free end of the beams.

Next, we test the finite metastructure to obtain the experimental bandgap. For open circuit condition, we plot the analytical dispersion curve for the experimental setup in Fig. 7. Then, we plot the experimental vibration frequency response curve of the system with highlighting the boundaries of the analytical bandgap by the dashed vertical lines in Fig. 8. The results indicate that the experimental bandgap lies within the analytical bandgap; however, there are multiple modes appearing in the middle of the bandgap. These modes are localized modes and are due to the low number of cells and existing boundary conditions. Therefore, these modes should be eliminated with increasing the number of cells in the model. To experimentally investigate the effect of energy harvesting on the boundaries of the bandgap, we plot the vibration frequency response curve of the finite structure in Fig. 9. As it was shown analytically, the shunted load resistor has no observaly effect on the bandgap size. Therefore, utilizing metastructure for energy harvesting applications does not degrade metastructure performance in terms of vibration attenuation.

CONCLUSION

In this paper, we investigated the effect of energy harvesting on vibration attenuation performance in locally resonant metastructures. The system was represented by an infinite chain of spring-mass systems. Each unit cell (i.e., spring mass system) is connected to an electromechanical local resonator. The electromechanical resonator was modeled as a spring-mass system and is shunted to a load resistor. A dispersion relation and the band structure of the system for different load resistor were derived analytically. The analytical results demonstrated that locally resonant metastructures can be employed to harvest electric power without degrading the vibration attenuation performance for a weakly electromechanical coupling case. However, the load resistor reduces the attenuation constant inside the bandgap. Nevertheless, extremely strong coupling can deform the band structure and merge the dispersion curves of optical and accoustics mode. Experiments were conducted on a finite structure to demonstrate the observed phenomena for a weakly electromechanical coupling case. The experimental results indicated the exsitance of bandgap in the frequency response curve although the tested structure was finite. However, the effect of finite struc-

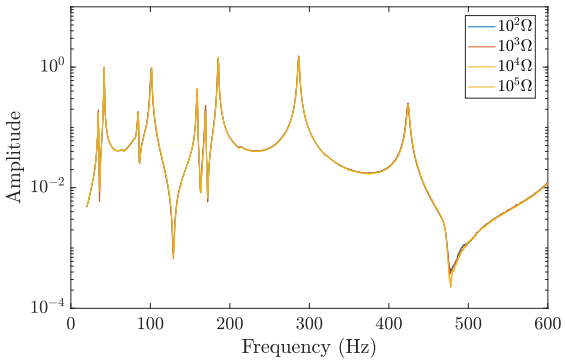

FIGURE 9: The effect of electromechanical coupling on the vibration frequency response curve for a chain with electromechanical resonator with parameters in the experimental setup: $\omega_d = 790$, $\omega_n = 1266$ rad/s^2, $k_1 = 6.788 \times 10^5$, $\bar{k} = 0.3581$.

ture and boundary conditions appeared as localized modes inside the bandgap. Moreover, the test demonstrated that harvesting electrical power does not change the bandgap size.

ACKNOWLEDGMENT

This work is supported in part by the National Science Foundation (NSF) Grant ECCS-1944032: CAREER: Towards a Self-Powered Autonomous Robot for Intelligent Power Lines Vibration Control and Monitoring.

REFERENCES

[1] Hussein, M. I., Leamy, M. J., and Ruzzene, M., 2014. "Dynamics of phononic materials and structures: Historical origins, recent progress, and future outlook". *Applied Mechanics Reviews,* ***66***(4), p. 040802.

[2] Bertoldi, K., Vitelli, V., Christensen, J., and van Hecke, M., 2017. "Flexible mechanical metamaterials". *Nature Reviews Materials,* ***2***(11), p. 17066.

[3] Sigalas, M. M., and Economou, E. N., 1992. "Elastic and acoustic wave band structure". *Journal of Sound Vibration,* ***158***, pp. 377–382.

[4] Sigalas, M., and Economou, E. N., 1993. "Band structure of elastic waves in two dimensional systems". *Solid state communications,* ***86***(3), pp. 141–143.

[5] Kushwaha, M. S., Halevi, P., Dobrzynski, L., and Djafari-Rouhani, B., 1993. "Acoustic band structure of periodic elastic composites". *Physical review letters,* ***71***(13), p. 2022.

[6] Kushwaha, M. S., Halevi, P., Martinez, G., Dobrzynski, L., and Djafari-Rouhani, B., 1994. "Theory of acoustic band structure of periodic elastic composites". *Physical Review B,* ***49***(4), p. 2313.

[7] Vasseur, J., Djafari-Rouhani, B., Dobrzynski, L., Kushwaha, M., and Halevi, P., 1994. "Complete acoustic band gaps in periodic fibre reinforced composite materials: the carbon/epoxy composite and some metallic systems". *Journal of Physics: Condensed Matter,* ***6***(42), p. 8759.

[8] Kushwaha, M. S., 1996. "Classical band structure of periodic elastic composites". *International Journal of Modern Physics B,* ***10***(09), pp. 977–1094.

[9] Liu, Z., Zhang, X., Mao, Y., Zhu, Y., Yang, Z., Chan, C. T., and Sheng, P., 2000. "Locally resonant sonic materials". *science,* ***289***(5485), pp. 1734–1736.

[10] Achaoui, Y., Laude, V., Benchabane, S., and Khelif, A., 2013. "Local resonances in phononic crystals and in random arrangements of pillars on a surface". *Journal of Applied Physics,* ***114***(10), p. 104503.

[11] Liu, L., and Hussein, M. I., 2012. "Wave motion in periodic flexural beams and characterization of the transition between bragg scattering and local resonance". *Journal of Applied Mechanics,* ***79***(1), p. 011003.

[12] Thorp, O., Ruzzene, M., and Baz, A., 2001. "Attenuation and localization of wave propagation in rods with periodic shunted piezoelectric patches". *Smart Materials and Structures,* ***10***(5), p. 979.

[13] Airoldi, L., and Ruzzene, M., 2011. "Wave propagation control in beams through periodic multi-branch shunts". *Journal of Intelligent Material Systems and Structures,* ***22***(14), pp. 1567–1579.

[14] Casadei, F., Delpero, T., Bergamini, A., Ermanni, P., and Ruzzene, M., 2012. "Piezoelectric resonator arrays for tunable acoustic waveguides and metamaterials". *Journal of Applied Physics,* ***112***(6), p. 064902.

[15] Bergamini, A., Delpero, T., Simoni, L. D., Lillo, L. D., Ruzzene, M., and Ermanni, P., 2014. "Phononic crystal with adaptive connectivity". *Advanced Materials,* ***26***(9), pp. 1343–1347.

[16] Zhou, W., Wu, Y., and Zuo, L., 2015. "Vibration and wave propagation attenuation for metamaterials by periodic piezoelectric arrays with high-order resonant circuit shunts". *Smart Materials and Structures,* ***24***(6), p. 065021.

[17] Hu, G., Tang, L., Banerjee, A., and Das, R., 2017. "Metastructure with piezoelectric element for simultaneous vibration suppression and energy harvesting". *Journal of Vibration and Acoustics,* ***139***(1), p. 011012.

[18] Shen, L., Wu, J. H., Zhang, S., Liu, Z., and Li, J., 2015. "Low-frequency vibration energy harvesting using a locally resonant phononic crystal plate with spiral beams". *Modern Physics Letters B,* ***29***(01), p. 1450259.

[19] Hu, G., Tang, L., and Das, R., 2017. "Metamaterial-inspired piezoelectric system with dual functionalities: energy harvesting and vibration suppression". In Active

and Passive Smart Structures and Integrated Systems 2017, Vol. 10164, International Society for Optics and Photonics, p. 101641X.

[20] Hu, G., Tang, L., and Das, R., 2018. "Internally coupled metamaterial beam for simultaneous vibration suppression and low frequency energy harvesting". *Journal of Applied Physics,* ***123***(5), p. 055107.

[21] Li, Y., Baker, E., Reissman, T., Sun, C., and Liu, W. K., 2017. "Design of mechanical metamaterials for simultaneous vibration isolation and energy harvesting". *Applied Physics Letters,* ***111***(25), p. 251903.

[22] Tol, S., Degertekin, F., and Erturk, A., 2017. "Phononic crystal luneburg lens for omnidirectional elastic wave focusing and energy harvesting". *Applied Physics Letters,* ***111***(1), p. 013503.

[23] Narisetti, R. K., Leamy, M. J., and Ruzzene, M., 2010. "A perturbation approach for predicting wave propagation in one-dimensional nonlinear periodic structures". *Journal of Vibration and Acoustics,* ***132***(3), p. 031001.

[24] Priya, S., and Inman, D. J. *Energy harvesting technologies*, Vol. 21. Springer.